Supplementary Information

1. General Information 2

2. Synthesis of Tetra(4-carboxyphenyl)porphine-Mn ligand 3

3. Synthetic conditions of the Catalyst 5

4. Structure of Hf-TCPP-Mn-MOL 7

5. Characterization of Hf-TCPP-Mn-MOL and Hf-TCPP-Mn-MOL-Sc 8

6. Characterization of Hf-TCPP-MOL and Hf-TCPP-MOL-Sc 11

7. Metal loadings of various catalyst samples determined by ICP-OES analysis 14

8. Control experiment 15

9. XPS analysis of the Hf-TCPP-Mn-MOL-Sc/ Hf-TCPP-MOL-Sc catalyst 16

10. Analysis of styrene oxidation products by gas chromatography (GC) 17

Reference 20

1. General Information

Chemicals. Manganese(II) Chloride Tetrahydrate (99%), meso-Tetra(4-carboxyphenyl)porphine (95%), Meso-Tetra(4-carboxyphenyl)porphine tetramethyl ester (95%), Hafnium (IV) chloride (99.9%, $HfCl_4$), 4-Methylanisole (99%) were purchased from J&K Scientific Co. and Ltd. N, N-dimethylformamide (DMF), formic acid (HCO_2H), tetrahydrofuran (THF), 1,2-dichloroethane were purchased from Sinopharm Chemical Reagent Co. Commercially available chemicals and reagents were used without further purification unless otherwise stated.

General experimental. The powder X-ray diffraction (PXRD) patterns were performed on Rigaku IV diffractometer with Cu Kα radiation (λ = 1.54178 Å). Transmission electron microscopy (TEM) images were obtained on JEOL2100 and Tecnai F30 High-Resolution Transmission Electron Microscopy and JEOL 1400. The sample was prepared by dispersing it in ethanol via a wet method, followed by ultrasonication for 20 minutes. The resulting dispersion was then deposited onto a copper grid and dried by evaporation on filter paper prior to analysis. The ^{1}H-NMR spectra were acquired on Bruker Avance II 500 M spectrometers. Thermogravimetric analysis (TGA) was conducted with a Netzsch TG209F1 instrument, where samples placed in an Al_2O_3 crucible were heated from 30 °C to 800 °C under an air flow. For inductively coupled plasma-optical emission spectroscop (ICP-OES) analysis, sample digestion and dilution were performed prior to measurement on an Agilent Technologies system. The surface chemical state of the catalyst was analyzed by X-ray photoelectron spectroscopy (XPS) on a Kratos AXIS Ultra DLD instrument. UV-Vis spectra were recorded using an Agilent Cary 60 spectrophotometer.

2. Synthesis of Tetra(4-carboxyphenyl)porphine-Mn ligand

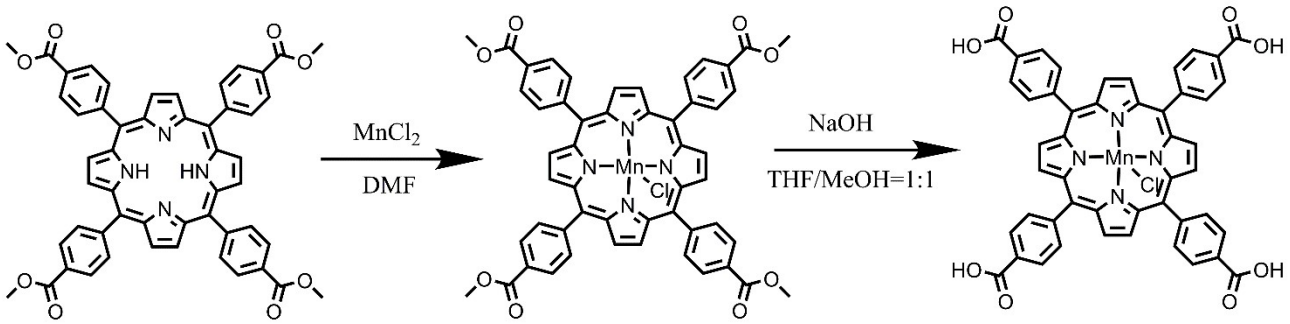

Fig. S1 Synthesis of Tetra(4-carboxyphenyl)porphine-Mn ligand.

A mixture of 5,10,15,20-meso-tetra[4-(methoxycarbonyl)phenyl]porphyrin (1.71 g, 2 mmol) and $MnCl_2$ (989.55 mg, 5 mmol) was dissolved in 120 mL of DMF. The solution was stirred until homogeneous and then refluxed at 140 °C for 12 h. After cooling to room temperature, the reaction mixture was extracted with dichloromethane and washed several times with water to remove residual DMF and salts. The organic phase was dried over anhydrous $MgSO_4$, and the solvent was removed under reduced evaporation to afford a dark green solid (1.63 g, yield: 87.14%).

The obtained ester intermediate (1.40 g, 1.5 mmol) was dissolved in a mixed solvent of THF (50 mL) and methanol (50 mL). An aqueous solution (40 mL) of KOH (841.5 mg, 15 mmol) was slowly added, and the mixture was refluxed for 12 h. After completion of the reaction, THF and methanol were evaporated under reduced pressure. Water (50 mL) was added, and the solution was acidified with 1 M HCl until no further precipitation was observed. The resulting solid was collected, washed with water, and dried under vacuum to give a dark green solid (0.99 g, yield: 75.07%).

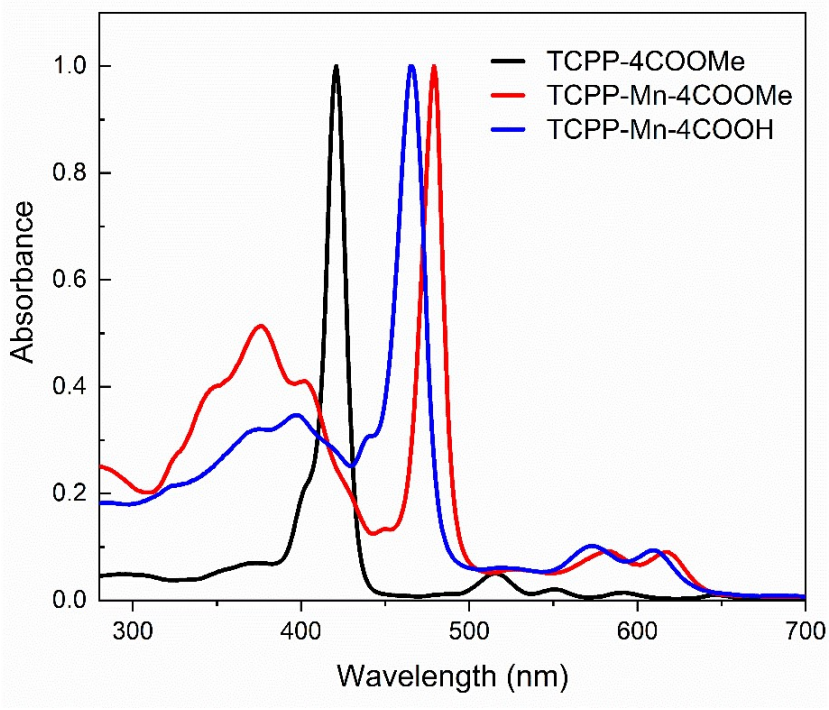

Fig. S2 Comparative UV-Vis spectra of the free-base and manganese porphyrin derivatives.

3. Synthetic conditions of the Catalyst

The synthesis conditions for Hf-TCPP-Mn-MOL (porphyrin-based metal–organic layer) were optimized by systematically varying the amount of formic acid (HCO_2H) introduced into the reaction system. The addition of formic acid serves not only as a capping agent to reduce surface energy but also as a coordination-modulating species. As shown in **Fig. S3** and **Fig. S4** (Supporting Information), although the resulting MOL consistently exhibited a mixed phase comprising both flat and zigzag lattice configurations, synthesis conditions yielding well-defined PXRD patterns—particularly Condition 7—were successfully identified.

Synthesis of Hf-TCPP-Mn-MOL/TCPP-MOL. Hafnium tetrachloride ($HfCl_4$, 19.2 mg, 0.06 mmol) and the TCPP-Mn ligand (8.8 mg, 0.01 mmol) were dissolved in a mixed solvent of 1.6 mL N, N-dimethylformamide (DMF) and 0.66 mL deionized water. After complete dissolution, 0.75 mL of formic acid was added to the reaction mixture. The sealed pressure-resistant vial was heated at 120 °C for 2 days. After cooling, the brown solid product was isolated by centrifugation and washed five times with DMF to obtain the target material. The synthesis of Hf-TCPP-MOL was identical to that described above, except that the TCPP-Mn ligand was replaced with TCPP.

Synthesis of Hf-TCPP-Mn-MOL-Sc/TCPP-MOL-Sc. Scandium trifluoromethanesulfonate ($Sc(SO_3CF_3)_3$, 496 mg, 1 mmol) was dissolved in 10 mL of tetrahydrofuran (THF). To this solution, Hf-TCPP-Mn-MOL (0.15 mmol) was added. The resulting suspension was stirred at 60 °C for 12 h. The solid was then collected by centrifugation and washed six times with THF to remove any residual $Sc(SO_3CF_3)_3$. The synthesis of Hf-TCPP-MOL-Sc was identical to that described above, except that the TCPP-Mn-MOL was replaced with Hf-TCPP-MOL.

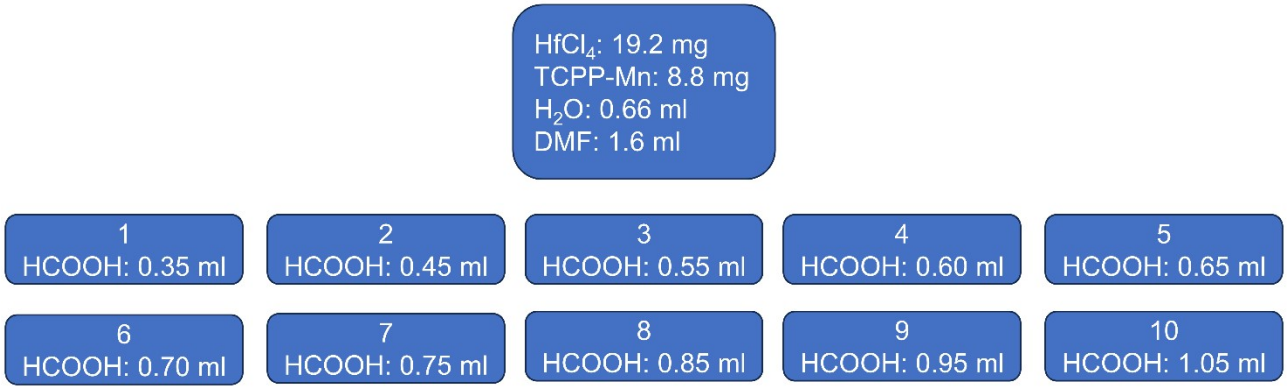

Fig. S3 Schematic diagram of the Hf-TCPP-Mn-MOL synthesis under different formic acid (HCOOH) volumes.

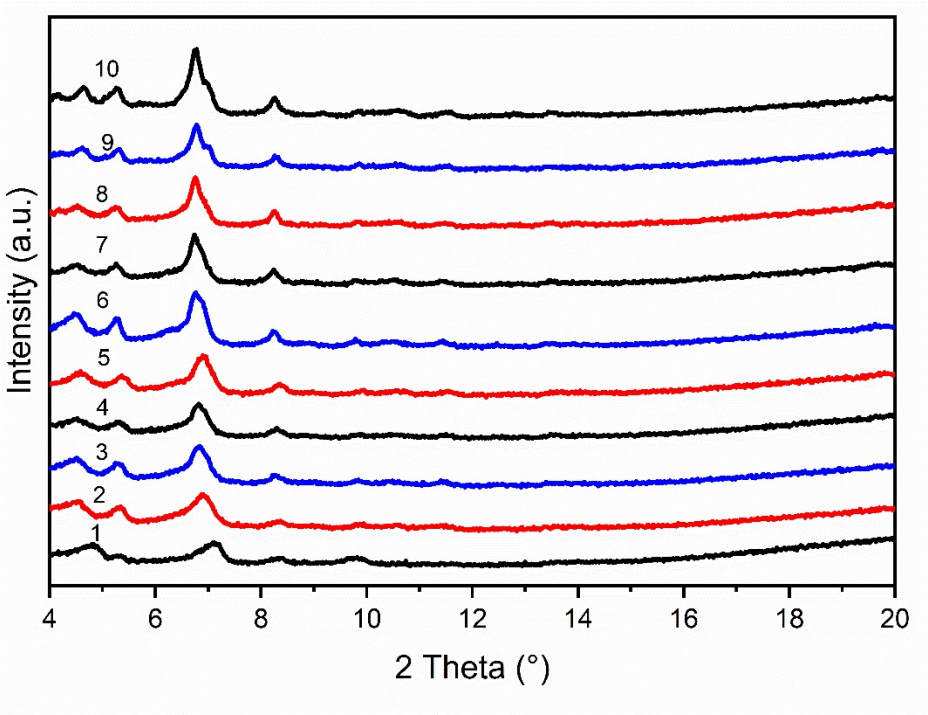

Fig. S4 PXRD patterns of Hf-TCPP-Mn-MOL samples synthesized with different volumes of formic acid (HCOOH) modulator.

4. Structure of Hf-TCPP-Mn-MOL

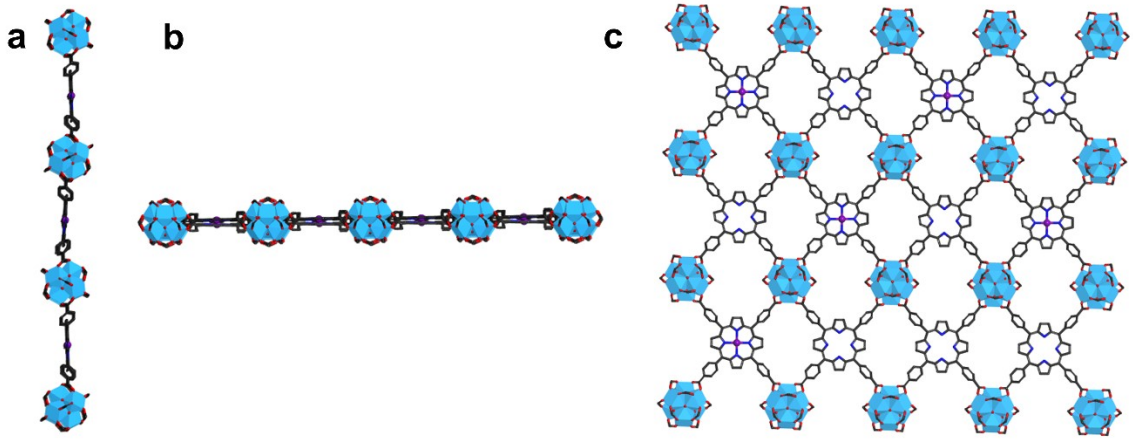

Fig. S5 The structure of the $[Hf_6(\mu_3\text{-}O)_4(\mu_3\text{-}OH)_4(\mu_1\text{-}OH)_2(\mu_1\text{-}H_2O)_2(HCO_2)_6([(TCPP)Mn])]$: viewed along the α axis(a). viewed along the b axis (b). topview of the monolayer (c).

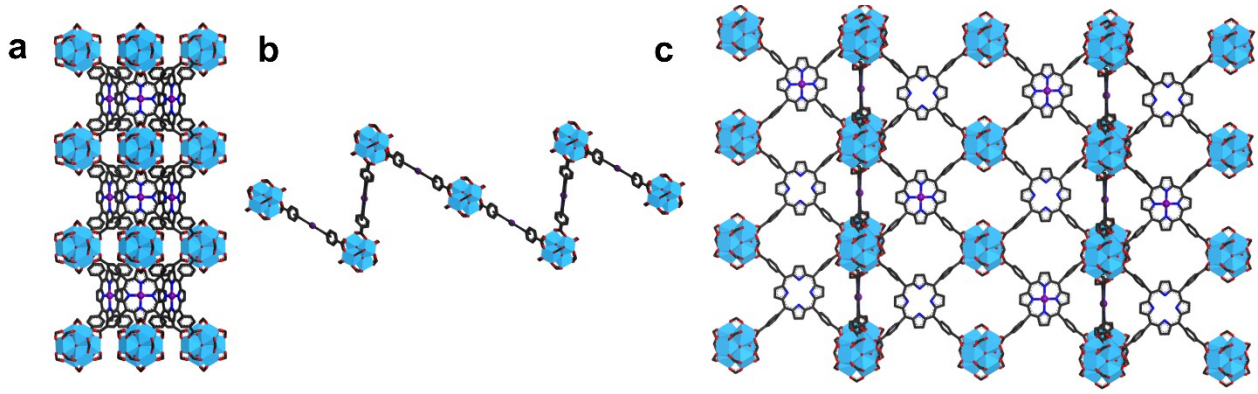

Fig. S6 The structure of the zig-zag monolayer: viewed along the α axis (a). viewed along the b axis (b). topview of the monolayer(c).

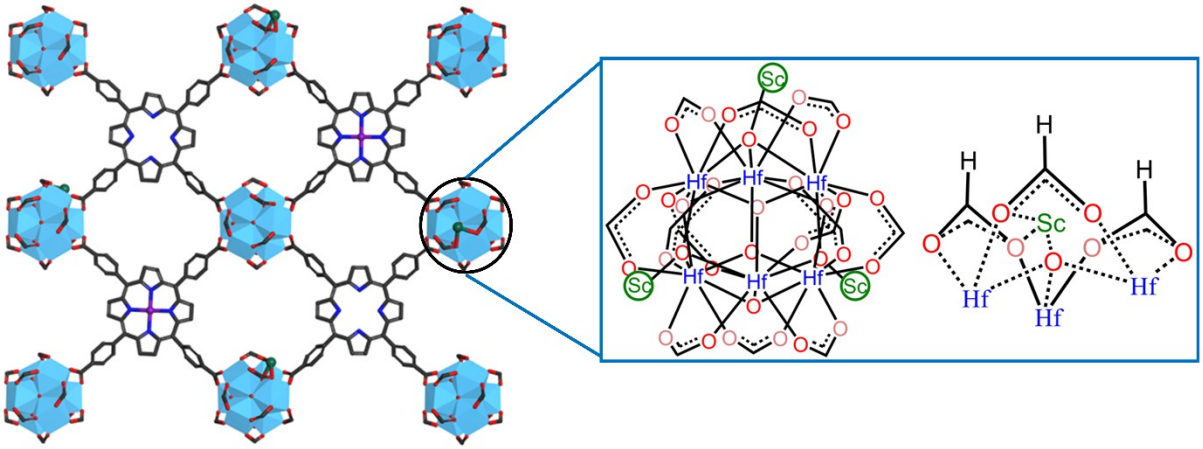

Fig. S7 Anchoring Sites of Sc^{3+} on the Hf_6 Secondary Building Unit.

5. Characterization of Hf-TCPP-Mn-MOL and Hf-TCPP-Mn-MOL-Sc

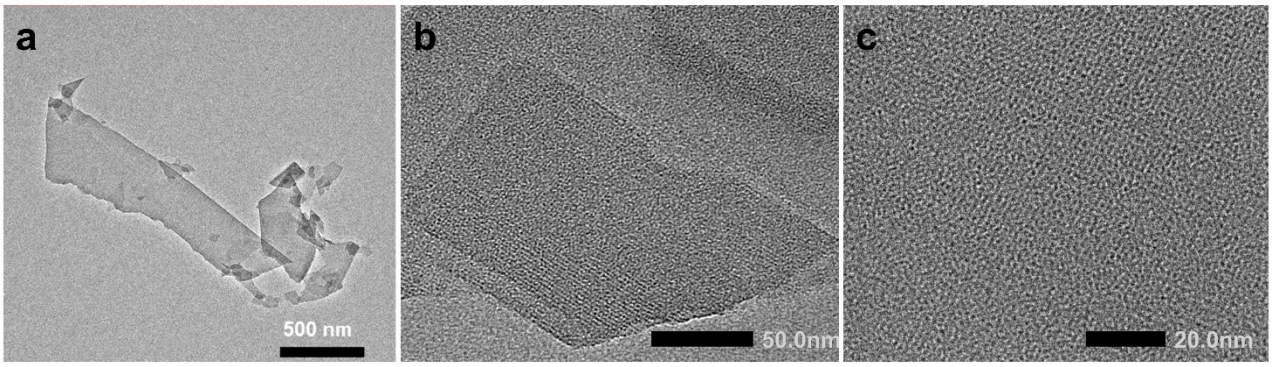

Fig. S8 TEM (a) and HRTEM (b, c) image of Hf-TCPP-Mn-MOL.

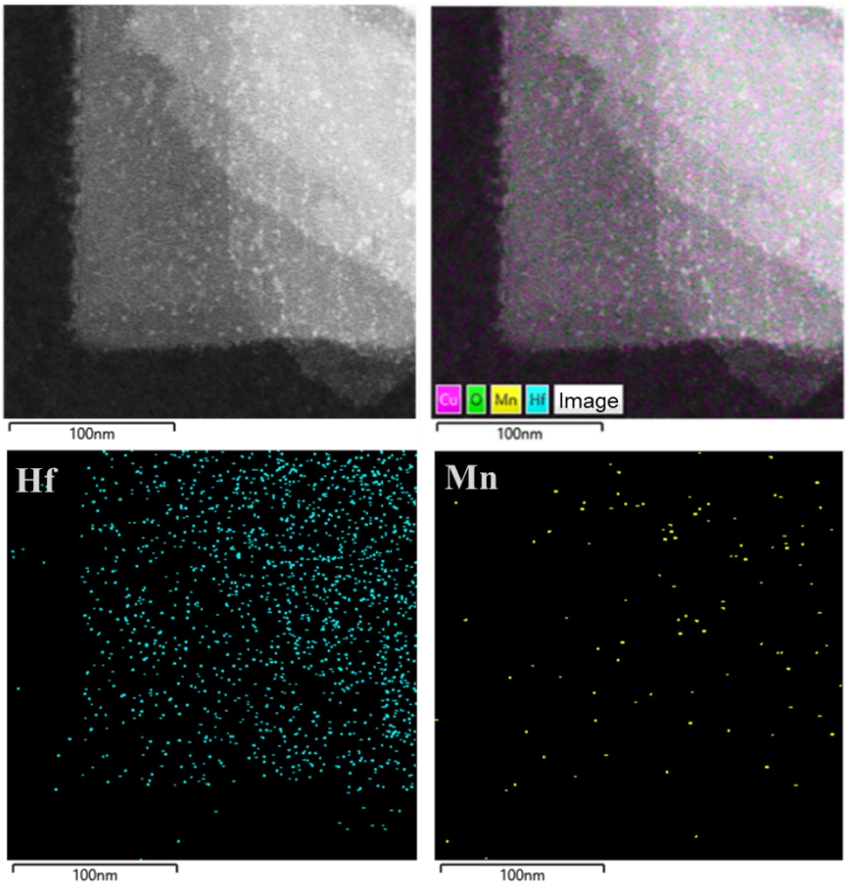

Fig. S9 Dark-field TEM image and the corresponding mapping analysis of Hf-TCPP-Mn-MOL.

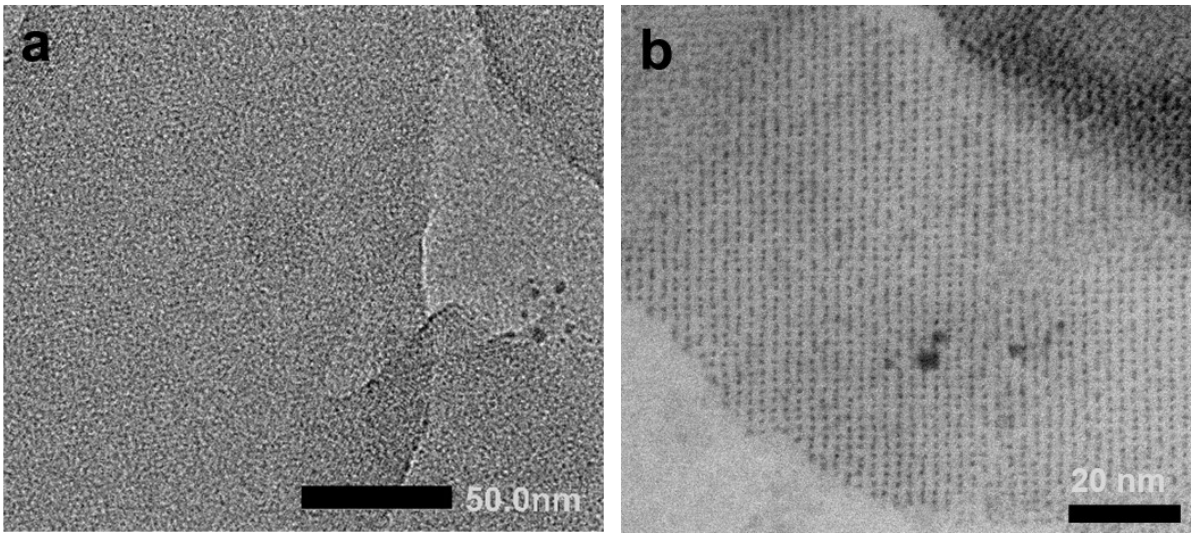

Fig. S10 HRTEM image of Hf-TCPP-Mn-MOL-Sc (a-b).

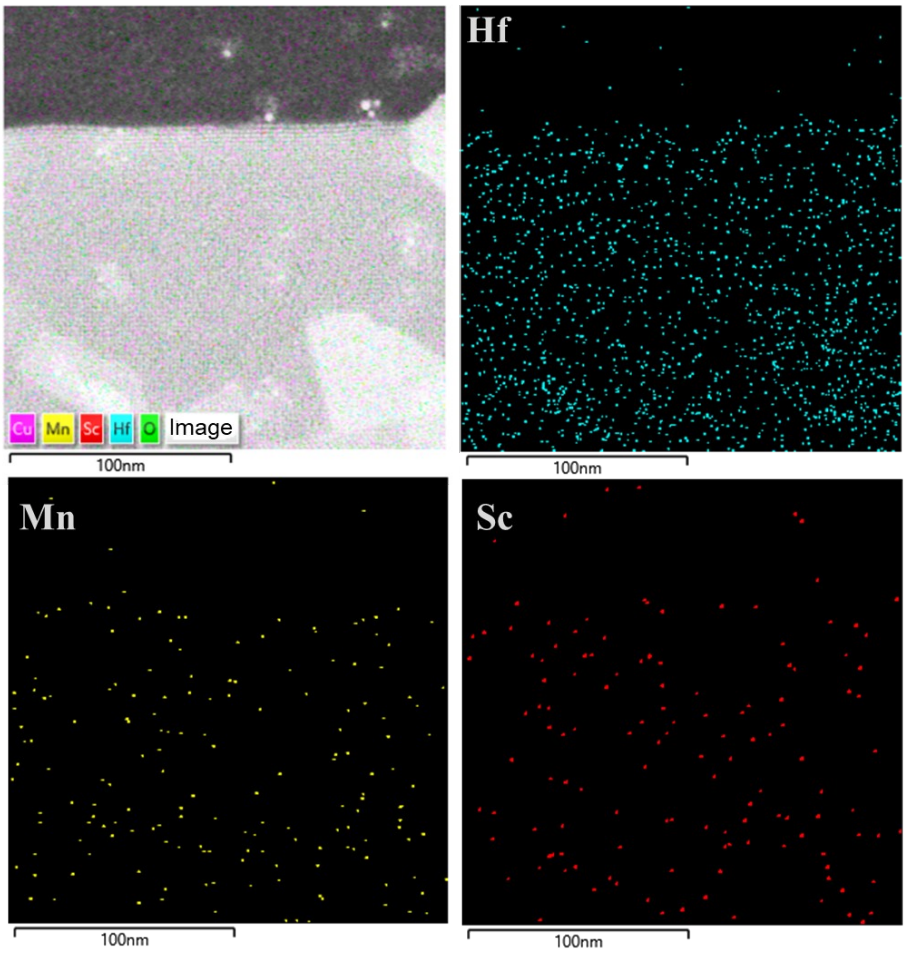

Fig. S11 Dark-field TEM image and the corresponding mapping analysis of Hf-TCPP-Mn-MOL-Sc.

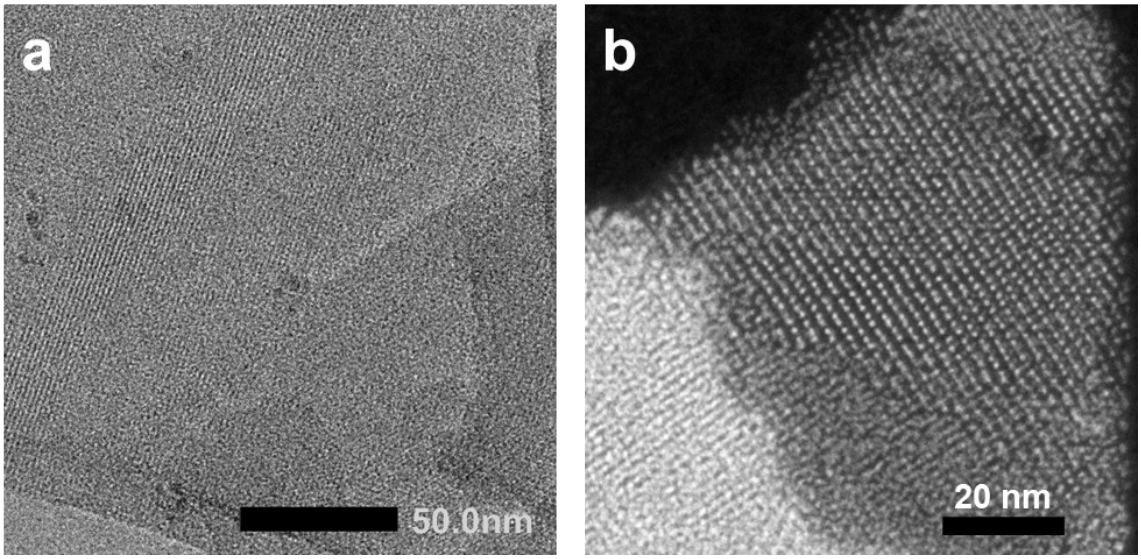

Fig. S12 HRTEM image of used TCPP-Mn-MOL-Sc (a-b).

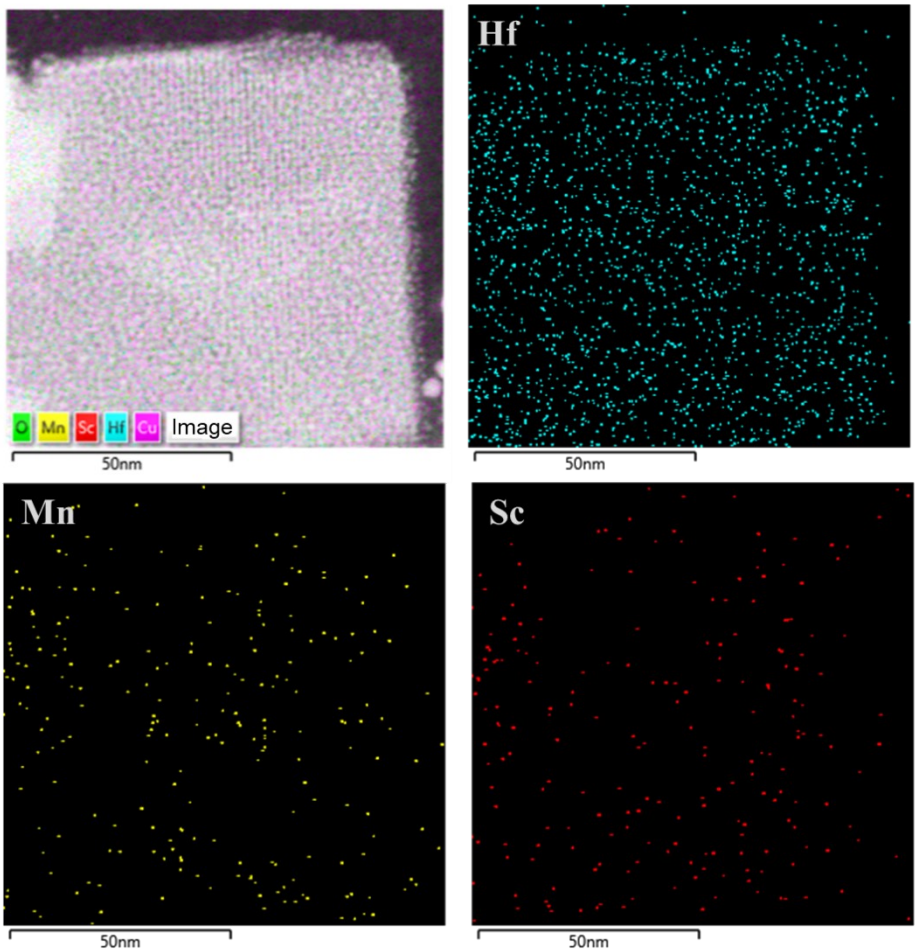

Fig. S13 Dark-field TEM image and the corresponding mapping analysis of used Hf-TCPP-Mn-MOL-Sc.

6. Characterization of Hf-TCPP-MOL and Hf-TCPP-MOL-Sc

The powder X-ray diffraction (PXRD) pattern of Hf-TCPP-MOL matches a combination of simulated patterns for the flat and zigzag monolayer models, suggesting that its actual structure may consist of a mixture of these two phases. Despite this complexity, the material retained its crystallinity and sheet-like morphology after the post-synthetic modification.

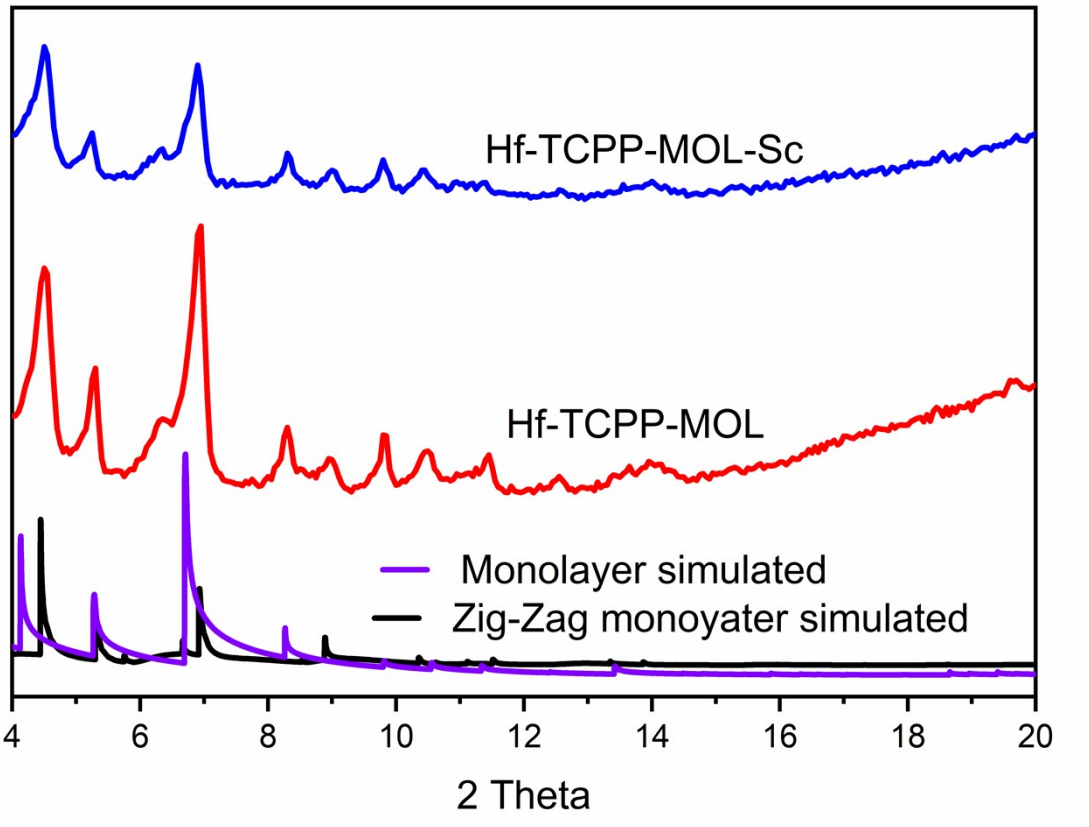

Fig. S14 PXRD pattern of Hf-TCPP-MOL and Hf-TCPP-MOL-Sc.

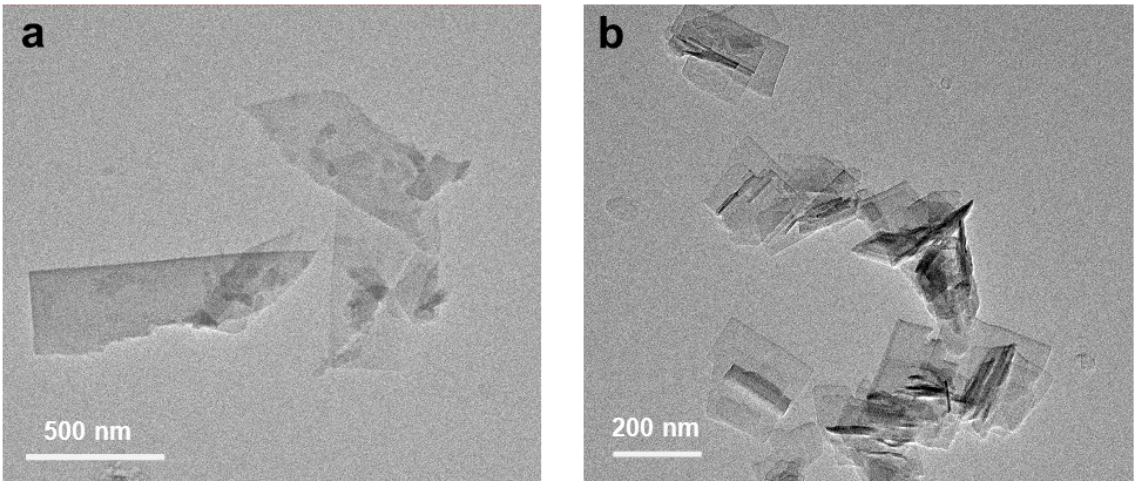

Fig. S15 TEM image of Hf-TCPP-MOL (a) and Hf-TCPP-MOL-Sc (b).

Elemental mapping performed by high-angle annular dark-field scanning transmission electron microscopy (HAADF-STEM) coupled with energy-dispersive X-ray spectroscopy (EDS) on Hf-TCPP-MOL-Sc confirmed the homogeneous distribution of Hf, and Sc throughout the sample.

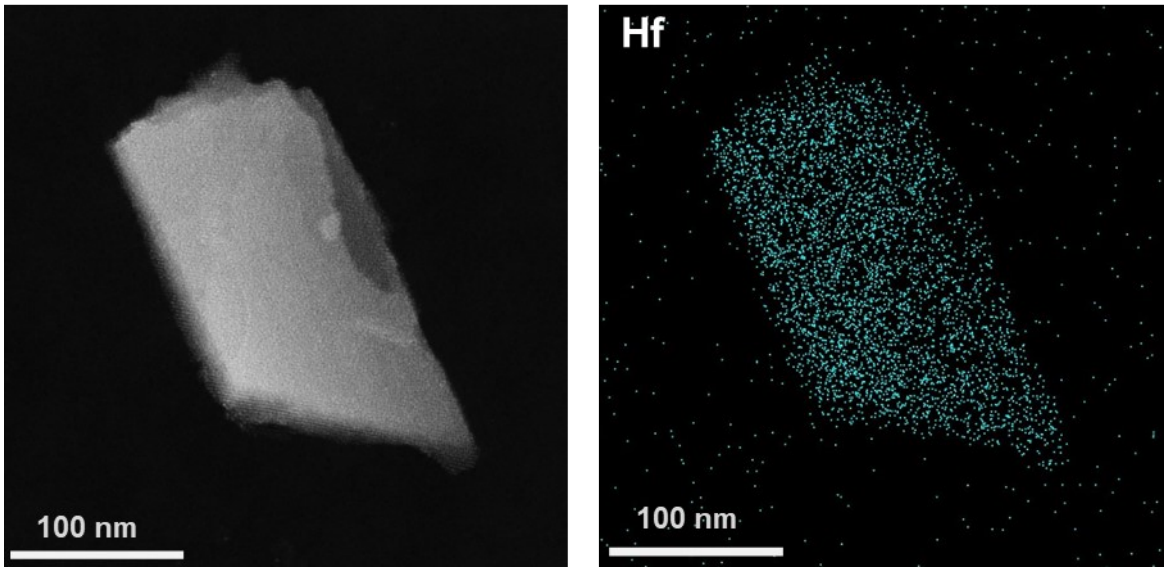

Fig. S16 Dark-field TEM image and the corresponding mapping analysis of Hf-TCPP-MOL.

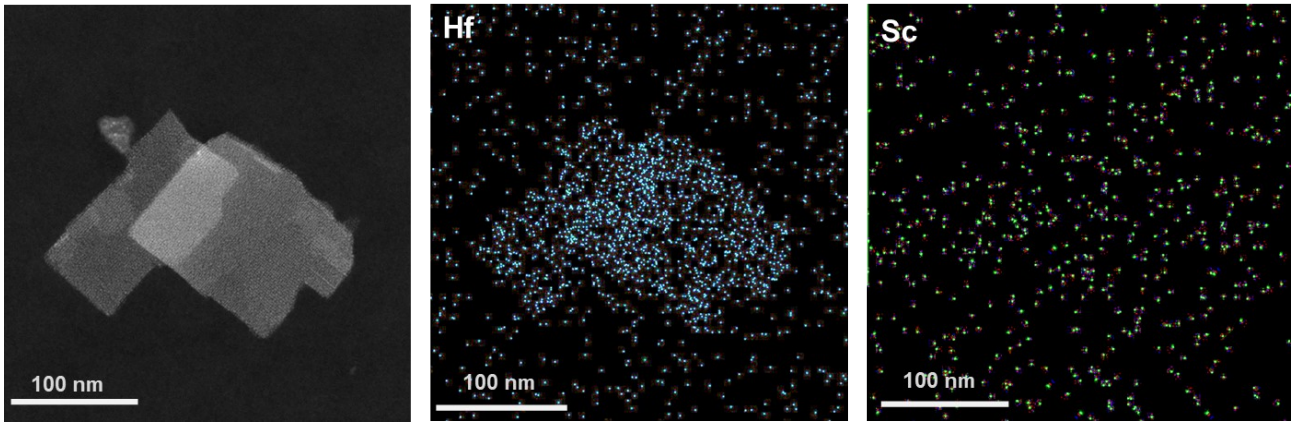

Fig. S17 Dark-field TEM image and the corresponding mapping analysis of Hf-TCPP-MOL-Sc.

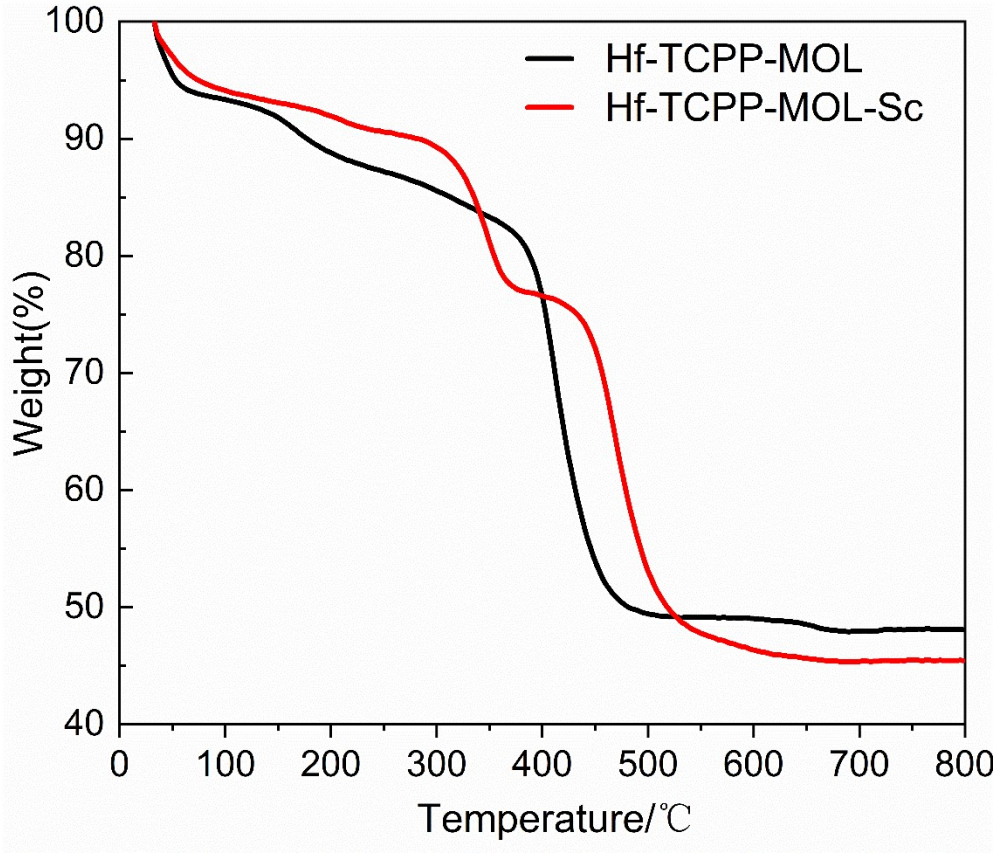

Fig. S18 TGA results of Hf-TCPP-MOL and Hf-TCPP-MOL-Sc.

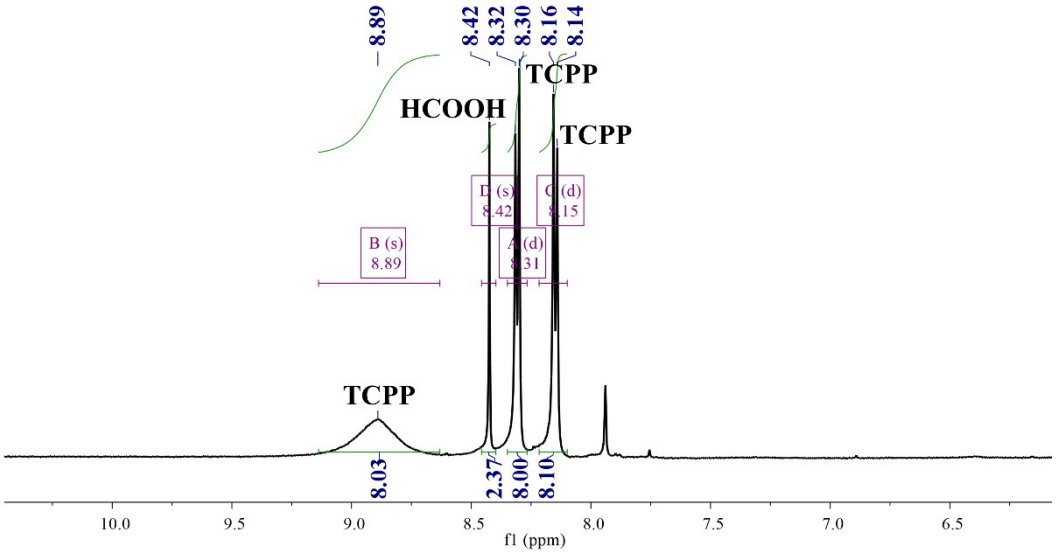

Fig. S19 ^{1}H NMR spectrum of Hf-TCPP-MOL after digestion in K_3PO_4/D_2O solution.

7. Metal loadings of various catalyst samples determined by ICP-OES analysis

Table S1 ICP-MS results of catalysts and control samples.

Sample	Mn(wt%)	Sc(wt%)	Mn/Hf (mol/mol)	Sc/Hf (mol/mol)	Mn/Sc (mol/mol)
TCPP-Mn-MOL	0.39		0.052		
TCPP-Mn-MOL-Sc	0.25	0.25	0.056	0.070	0.81
TCPP-MOL-Sc		0.22		0.057	
Used TCPP-Mn-MOL-Sc	0.31	0.37	0.053	0.077	0.69

8. Control experiment

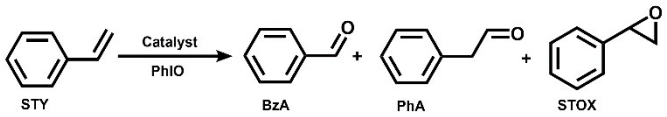

Table S2 Control of Product Yields in Styrene Oxidation-Rearrangement under Varied Conditions.

Catalyst	Temperature (℃)/time (h)	Yield (%)		
		BzA	PhA	STOX
Hf-TCPP-Mn-MOL	RT/2h→80℃/4h	2	32	57
Hf-TCPP-Mn-MOL[a]	RT/2h→80℃/4h	11	31	60
Hf-TCPP-Mn-MOL + Hf-TCPP-MOL-Sc	RT/2h→80℃/4h	2	84	/

Reaction conditions: catalyst (0.003 mmol), styrene (1 mmol), PhIO (0.15 mmol), 1,2-dichloroethane (5 mL). BzA: benzaldehyde. PhA: phenylacetaldehyde. STOX: styrene oxide. Reaction solution was degassed with N_2. [a]The reaction was performed under air. Yields were determined by gas chromatography (GC) using 4-methylanisole as an internal standard and calculated based on the starting amount of PhIO.

Table S3 Catalytic performance of Hf-TCPP-Mn-MOL-Sc for linear alkyl alkenes under standard conditions

Entry	Substrate	Product **1**	Yield (%)	Product **2**	Yield (%)
1	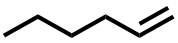	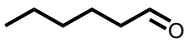	9	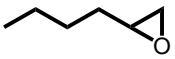	19
2	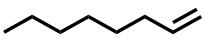		9	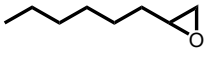	15

Reaction conditions: catalyst (0.003 mmol), substrate (1 mmol), PhIO (0.15 mmol), 1,2-dichloroethane (5 mL). The reaction solution was degassed and stirred at room temperature for 2 h, followed by 4 h at 80 °C. Yields were determined by ^{1}H-NMR spectroscopy using 4-methylanisole as an internal standard, with calculations based on the starting amount of PhIO.

9. XPS analysis of the Hf-TCPP-Mn-MOL-Sc/ Hf-TCPP-MOL-Sc catalyst

The X-ray photoelectron spectroscopy (XPS) analysis of Hf-TCPP-Mn-MOL-Sc shows Sc 2p peaks at approximately 403.3 eV and 407.9 eV, which are assigned to the Sc^{3+} $2p^{3/2}$ and $2p^{1/2}$ orbitals, respectively[1]. The Sc 2p and N 1s XPS regions are known to exhibit spectral overlap. Furthermore, the binding energies observed for the Mn 2p orbitals ($2p^{3/2}$ at 642.6 eV and $2p^{1/2}$ at 653.7 eV) are consistent with the chemical state of manganese in manganese(III) porphyrin complexes[2-4].

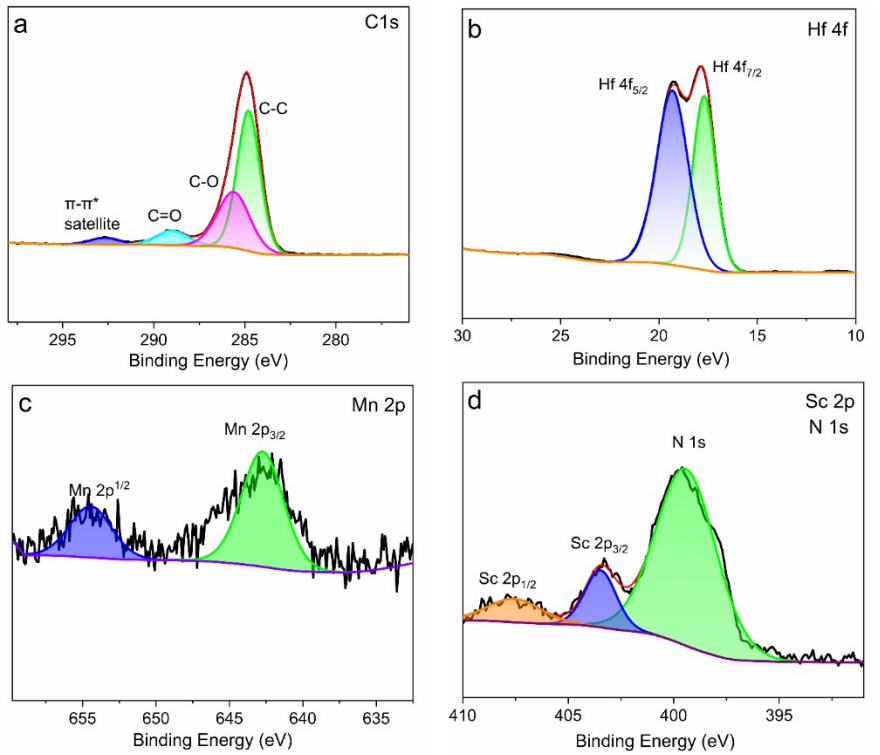

Fig. S20 XPS characterization of the Hf-TCPP-Mn-MOL-Sc catalyst, confirming the presence of C (a), and Hf (b), Mn (c), Sc and N (d) elements.

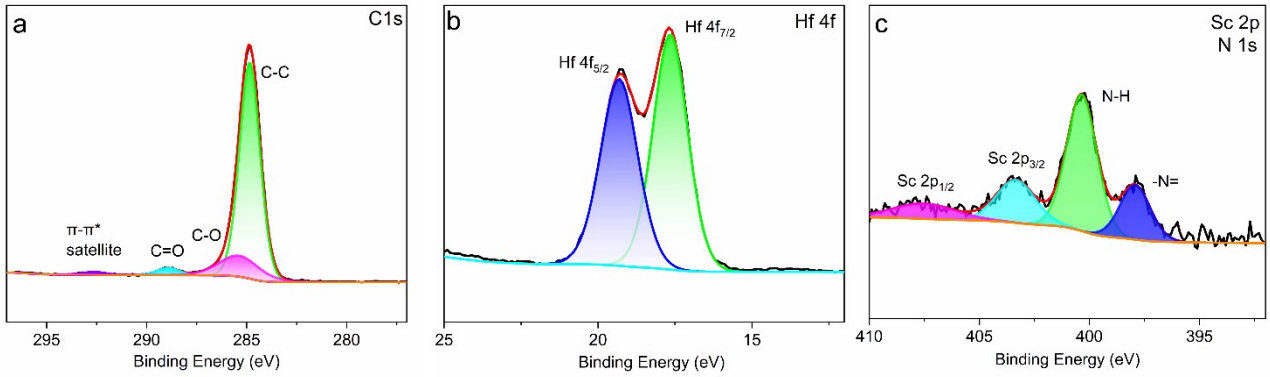

Fig. S21 XPS characterization of the Hf-TCPP-Mn-MOL-Sc catalyst, confirming the presence of C (a), and Hf (b), Sc and N (c) elements.

10. Analysis of styrene oxidation products by gas chromatography (GC)

Reactions were performed with styrene (1 mmol) and PhIO (0.15 mmol) in 1,2-dichloroethane (5 mL), except for entry (d) where styrene oxide was used as the substrate for the rearrangement reaction (no additional oxidant required). 4-Methylanisole was added as an internal standard after the reaction for analysis.

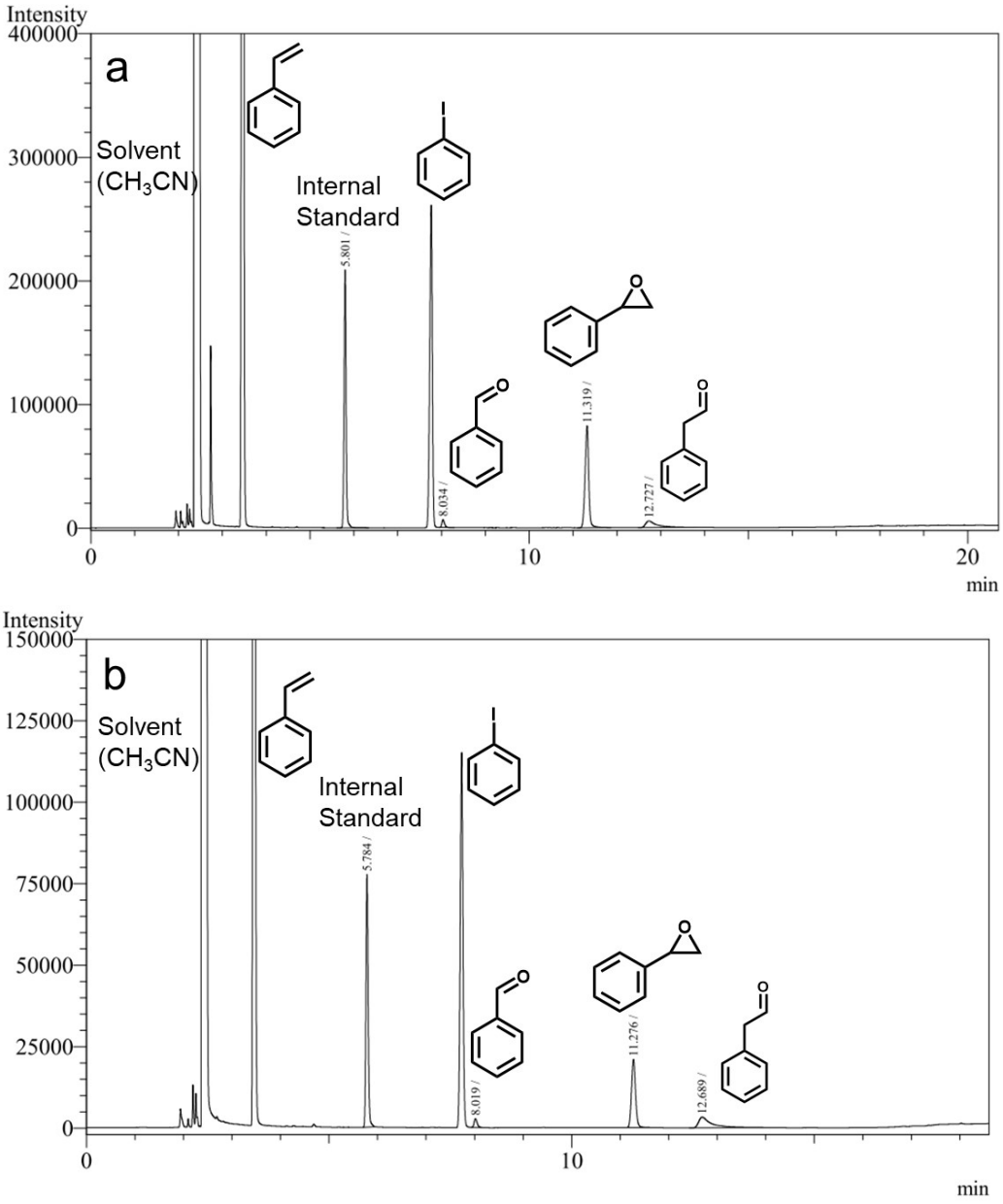

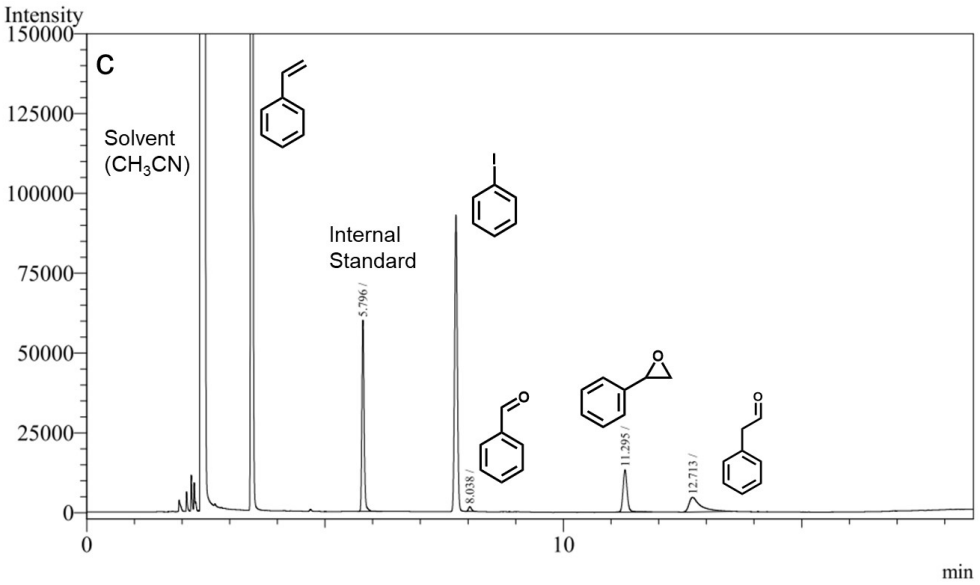
Intensity
150000
125000
100000
75000
50000
25000
0
c
Solvent
(CH3CN)
Internal
Standard
5.796
8.038
11.295
12.713
0
10
min

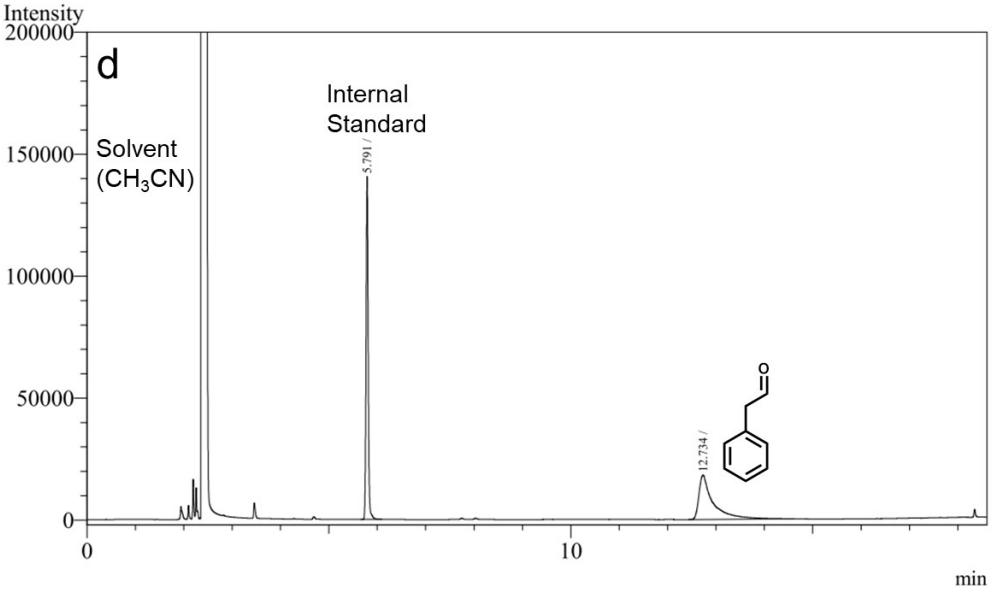
Intensity
200000
150000
100000
50000
0
d
Solvent
(CH3CN)
Internal
Standard
5.791
12.734
0
10
min

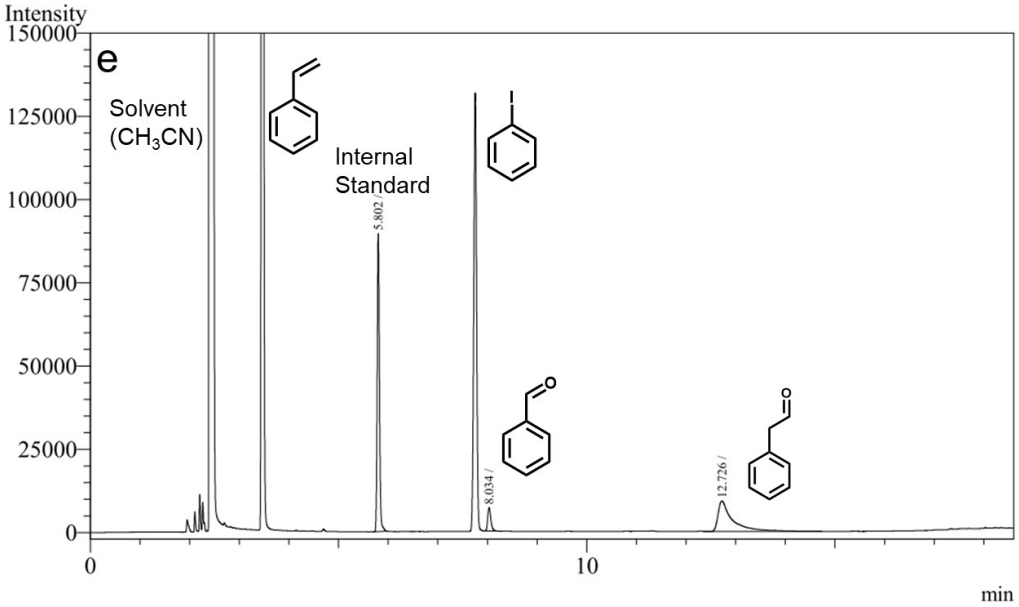
Intensity
150000
125000
100000
75000
50000
25000
0
e
Solvent
(CH3CN)
Internal
Standard
5.802
8.034
12.726
0
10
min

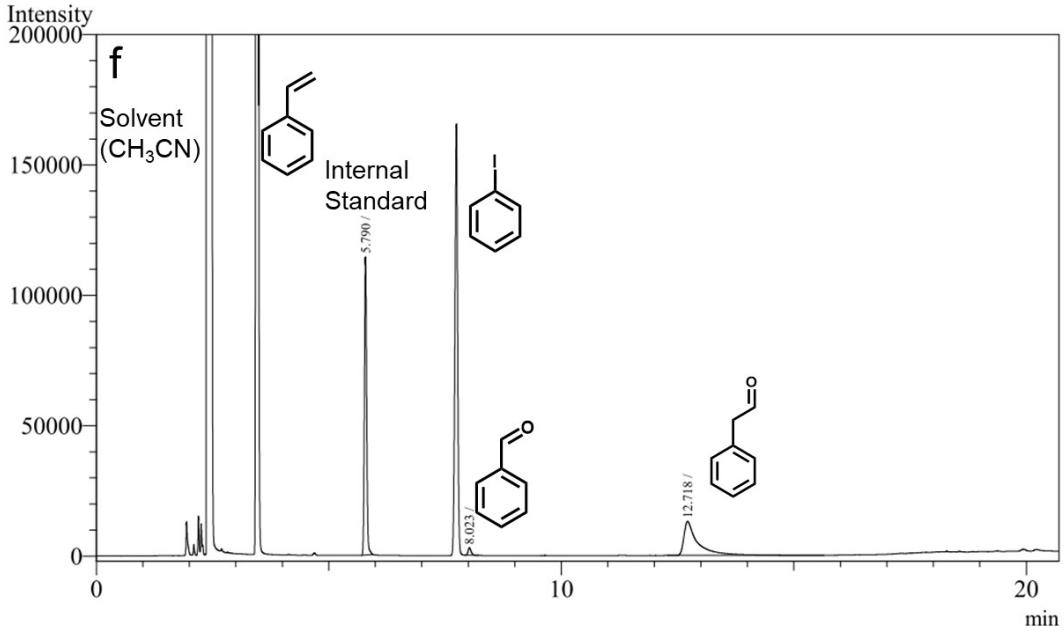

Fig. S22 GC Analysis of the Oxidation Products. The specific conditions for each catalytic entry are provided in the following descriptions. (a) The homogeneous catalyst Mn-TCPP-COOMe at room temperature for 2 h. (b) Hf-TCPP-Mn-MOL at room temperature for 2 h. (c) Hf-TCPP-Mn-MOL-Sc at room temperature for 2 h. (d) Rearrangement of styrene oxide catalyzed by Hf-TCPP-MOL-Sc at 80 ℃. (e) Hf-TCPP-Mn-MOL-Sc at room temperature for 2 h, followed by heating at 80 ℃. (f) Hf-TCPP-Mn-MOL-Sc under nitrogen-degassed conditions at room temperature for 2 h, followed by heating at 80 ℃.

Reference

1. V. V. Atuchin, M. S. Lebedev, S. A. Gromilov, I. V. Korolkov, T. V. Perevalov and I. P. Prosvirin, *J Electron Mater*, 2025, **54**, 4832-4845.
2. A. R. Antonangelo, C. G. Bezzu, N. B. McKeown and S. Nakagaki, *J Catal*, 2019, **369**, 133-142.
3. A. Kaplan, E. Korin and A. Bettelheim, *Eur J Inorg Chem*, 2014, **2014**, 2288-2295.
4. F. Yang, S. Y. Gao, C. R. Xiong, H. Q. Wang, J. Chen and Y. Kong, *Chinese J Catal*, 2015, **36**, 1035-1041.